

Full counting statistics for electron transport in periodically driven quantum dots

Thomas D. Honeychurch and Daniel S. Kosov

College of Science and Engineering, James Cook University, Townsville, QLD, 4811, Australia

Time-dependent driving influences the quantum and thermodynamic fluctuations of a system, changing the familiar physical picture of electronic noise which is an important source of information about the microscopic mechanism of quantum transport. Giving access to all cumulants of the current, the full counting statistics (FCS) is the powerful theoretical method to study fluctuations in nonequilibrium quantum systems. In this paper, we propose the application of FCS to consider periodic driven junctions. The combination of Floquet theory for time dynamics and nonequilibrium counting-field Green's functions enables the practical formulation of FCS for the system. The counting-field Green's functions are used to compute the moment generating function, allowing for the calculation of the time-averaged cumulants of the electronic current. The theory is illustrated using different transport scenarios in model systems.

I. INTRODUCTION

Time-dependent phenomena play an important part in the investigation and application of nanoscale electronics. The dynamical response of a junction to the modulation of a voltage or to the irradiation by a light source offers intriguing means of probing and controlling the system's dynamics¹. Applications include optically irradiated nanoscale junctions^{2,3}, electron pumping⁴⁻⁶, pump-probe spectroscopy^{7,8}, and AC current rectification^{9,10}. The exploration of time-dependent phenomena has a long history^{1,11}, which mostly centers on periodic drivings, typically induced with microwave radiation. For periodic driving, the explanation of photon-assisted transport (PAT) is often invoked: electrons, moving between regions under periodic driving, are observed to undergo inelastic tunneling events, with the absorption and emission of quanta of energy given by the driving frequency¹. PAT has been realized within many systems^{2,3,12}, and has undergone extensive theoretical investigation¹.

Many approaches have been developed to deal with driving within transport settings. Approaches include Floquet and scattering theories¹³⁻²¹, quantum master equations^{22,23}, nonequilibrium Green's functions (NEGF) based approaches²⁴⁻⁴⁵, and the evolution operator method⁴⁶⁻⁴⁸.

The discrete nature of the charge carrier results in irrepressible current fluctuations. These current fluctuations can contain information about the nature of the junction. For systems with explicit time dependence, understanding current fluctuations is crucial for metrological and performance reasons^{23,49}. Noise has been investigated with Floquet theories^{15,50}, NEGFs⁵¹⁻⁵⁷, and Floquet master-equation approaches⁵⁸.

Full counting statistics (FCS) allows the calculation of higher cumulants of the current in a rather concise and systematic manner. The theory of FCS was first introduced by Levitov and Lesovik^{59,60} in a scattering theory framework via the explicit inclusion of a measuring device in the theoretical setup, which has since been extended to a general quantum mechanical variable⁶¹ and applied to various transport scenarios⁶². For periodically

driven systems, FCS has been coupled within scattering theory⁶³⁻⁶⁵ and master-equation approaches^{5,66,67} with various investigated periodically driven systems.

NEGFs have proved indispensable in calculating FCS in quantum conductors with electron-phonon⁶⁸⁻⁷² and electron-electron^{73,74} interactions, and it has been applied to study fluctuations in the transient regime⁷⁴⁻⁷⁶. Recently, Yadalam and Harbola used FCS NEGFs to study charge pumping through a driven quantum dot^{4,5}.

The NEGF extension of FCS to quantum conductors with arbitrary time-periodic driving of the leads remains the challenging theoretical problem and has not been accomplished yet—this is the main goal of our paper. The need for a counting field complicates derivations within a time-dependent setting, as the equations of motion for the Green's functions become unwieldy integro-differential equations within the Keldysh-Schwinger space. In this paper, using Floquet Green's functions^{6,33,77,78}, we investigate full counting statistics for modeling systems with periodic driving of the leads. The periodicity within the system's dynamics allows for the Green's functions of the system to be cast as Fourier series. This allows for the recasting of the equations of motion in terms of matrix equations of infinite dimension, which are truncated at a particular point. Truncating the matrices amounts to truncating the Fourier series describing the Green's functions of the system. This approximation is well behaved and is applicable to situations of both strong and weak coupling to the leads, relative to the chosen driving frequency.

The method was applied to a single resonant level and a T-shaped double-level system. In both cases, the left lead underwent the sinusoidal driving of its energies. This results in photon-assisted transport being observed within the current cumulants, most notably resulting in additional noise in particular cases. For the T-shaped junction, Fano-resonance effects were found to manifest in the peaks generated by the driving. This was explained by considering the bonding and anti-bonding levels of the central molecule.

This paper is organized as follows. Section II describes the use of Floquet Green's functions to solve the equations of motion in an FCS context. In Sec. III, the

method is applied to the given systems. In Sec. IV, the results of the paper are summarized. Natural units for quantum transport are used throughout the paper, with \hbar , e , and k_B set to unity.

II. THEORY

A. General considerations

Within the investigation, the Hamiltonian for a central region (i.e., the molecule) connected to two macroscopic leads is given by

$$H(t) = H_C(t) + H_L(t) + H_R(t) + H_{CL}(t) + H_{CR}(t), \quad (1)$$

where H_C is the Hamiltonian of the molecule, H_L and H_R are the Hamiltonians of the left and right leads, and $H_{CL/R}$ is the interaction between the central region and the left/right lead, respectively.

We consider the electrons within the central region to be noninteracting:

$$H_C = \sum_{ij} h_{ij}(t) d_i^\dagger d_j, \quad (2)$$

where d_i^\dagger (d_i) creation (annihilation) operators are for an electron in the single-particle state i .

The left and right leads are modeled as macroscopic reservoirs of noninteracting electrons,

$$H_L + H_R = \sum_{k,\alpha=L,R} \epsilon_{k\alpha}(t) c_{k\alpha}^\dagger c_{k\alpha}, \quad (3)$$

where $c_{k\alpha}^\dagger$ ($c_{k\alpha}$) creates (annihilates) an electron in the single-particle state k of either the left ($\alpha = L$) or the right ($\alpha = R$) lead. The coupling between the central region and left and right leads is given by the tunneling interaction

$$H_{CL} + H_{CR} = \sum_{i,k,\alpha=L,R} \left[t_{k\alpha i}(t) c_{k\alpha}^\dagger d_i + \text{H.c.} \right], \quad (4)$$

where $t_{k\alpha i}(t)$ is the time-dependent tunneling amplitude between leads and central single-particle states.

Utilizing full counting statistics, we follow a common procedure^{4,73}. The generating function,

$$\chi(\lambda_L, t_c, t_0) = \langle e^{-i\lambda_L N_L(t_c)} e^{i\lambda_L N_L(t_0)} \rangle, \quad (5)$$

allows for the calculation of the charge that leaves the left lead between times t_0 and t_c . Here, $N_L(t)$ is the occupation of the left lead within the Heisenberg picture. The cumulants of the above are given by

$$\langle \delta^n q(t_c, t_0) \rangle = (-i)^n \frac{\partial^n}{\partial \lambda_L^n} \ln \chi(\lambda_L, t_c, t_0) \Big|_{\lambda_L=0}. \quad (6)$$

By taking the first derivative with respect to the counting field, this result can be recast:

$$\begin{aligned} & -i \frac{\partial}{\partial \lambda_L} \ln [\chi(\lambda_L, t_c, t_0)] \\ &= \int_{t_0}^{t_c} dt \int_{t_0}^{t_c} dt' \text{Tr} \left[\Sigma_{<}^L(t, t') \mathbf{G}_{>}(t', t) \right. \\ & \quad \left. - \mathbf{G}_{<}(t, t') \Sigma_{>}^L(t', t) \right], \quad (7) \end{aligned}$$

where the Hamiltonian is modified by the appropriate counting field

$$H_{CL}^{\lambda_L}(t) = \sum_{i,k} t_{kL,i}(t) e^{-\frac{i}{2}\lambda_L(\tau)} c_{k\alpha}^\dagger d_i + t_{kL,i}^*(t) e^{\frac{i}{2}\lambda_L(\tau)} d_i^\dagger c_{k\alpha}, \quad (8)$$

and where $\lambda(\tau) = \pm\lambda_L$ on the forward and backward branches of the contour, respectively. Here, the Green's functions are projections of the contour Green's function with the addition of the counting field:

$$G_{i,j}(\tau, \tau') = -i \frac{\text{Tr} \left[\hat{\rho}_0 \text{T}_c \left(e^{-i \int_c V_h^{\lambda(\bar{\tau})}(\bar{\tau}) d\bar{\tau}} a_i(\tau) a_j^\dagger(\tau') \right) \right]}{\text{Tr} \left[\hat{\rho}_0 \text{T}_c \left(e^{-i \int_c V_h^{\lambda(\bar{\tau})}(\bar{\tau}) d\bar{\tau}} \right) \right]}, \quad (9)$$

where $V_h^{\lambda(t)}$ is the coupling between the leads and the central region within the interaction picture and the additional counting field [i.e. $V_h^{\lambda(t)} = H_{CL}^{\lambda(t)}(t) + H_{CR}(t)$]. The counting field modifies the lesser and greater lead self-energies such that $\Sigma_L^< \rightarrow \Sigma_L^< e^{i\lambda_L}$ and $\Sigma_L^> \rightarrow \Sigma_L^> e^{-i\lambda_L}$, while the other self-energy terms are unchanged.

Moving to real time, the contour Green's function is expressed in Schwinger-Keldysh space,

$$\hat{\mathbf{G}}(t, t') = \begin{pmatrix} \mathbf{G}^T(t, t') & \mathbf{G}^<(t, t') \\ \mathbf{G}^>(t, t') & \mathbf{G}^T(t, t') \end{pmatrix}, \quad (10)$$

with the Kadanoff-Baym equations following the standard definition:

$$\begin{aligned} \left(i \frac{\partial}{\partial t} - \mathbf{h}(t) \right) \check{\mathbf{G}}(t, t') - \int_{t_0}^{t_c} dt_1 \check{\Sigma}(t, t_1) \check{\mathbf{G}}(t_1, t') \\ = \delta(t - t'), \quad (11) \end{aligned}$$

with $\check{A}_{2,j}(t, t') = -\hat{A}_{2,j}(t, t')$.⁷⁹

B. Floquet Green's functions

The system's periodicity within time allows for objects of interest to be cast as Fourier series^{6,33,78}. For a given two-time object, the Fourier coefficients are calculated as

$$A(\omega, m) = \frac{1}{P} \int_0^P dT e^{-i\Omega m T} \int_{-\infty}^{\infty} d\tau e^{i\omega\tau} A(T, \tau), \quad (12)$$

where $T = \frac{t+t'}{2}$ and $\tau = t - t'$. Given the above, one can make judicious choices about how to express the Fourier coefficients of the Kadanoff-Baym equations, leading to the problem being cast as matrix equations of infinite dimension.

Here, we outline the procedure of transforming the convolutions into the multiplication of matrices³³. The simpler elements of the Kadanoff-Baym equations follow easily. Considering Eq. (12), we wish to find the Fourier coefficients of the following object:

$$C(t, t') = \int dt_1 A(t, t_1) B(t_1, t'), \quad (13)$$

given the periodicity of terms $A(t, t')$ and $B(t, t')$ around the central time, i.e., $T = \frac{t+t'}{2}$. One can begin the transformation of Eq. (13) by first taking the Wigner transformation:

$$\begin{aligned} C(T, \omega) &= \int_{-\infty}^{\infty} d\tau e^{i\omega\tau} C(t, t') \\ &= e^{-\frac{i}{2}(\partial_T^A \partial_\omega^B - \partial_\omega^A \partial_T^B)} A(T, \omega) B(T, \omega). \end{aligned} \quad (14)$$

The objects within Wigner space can be expressed as Fourier series, leading to the simple evaluation of the time derivative:

$$\begin{aligned} C(\omega, m) &= \sum_{n=0}^{\infty} e^{\frac{\Omega}{2}[n\partial_\omega^B - \partial_\omega^A(m-n)]} A(\omega, n) B(\omega, m-n) \\ &= \sum_{n=-\infty}^{\infty} A\left(\omega + \frac{\Omega}{2}(n-m), n\right) B\left(\omega + \frac{\Omega}{2}n, m-n\right). \end{aligned} \quad (15)$$

Introducing $\omega \rightarrow \omega + l\Omega/2$, where l is an integer, and making use of the notation $\check{G}(\omega + \frac{\Omega}{2}l, m) \rightarrow \check{G}_{l,m}$, the above becomes

$$\begin{aligned} C_{l,m} &= \sum_{n=-\infty}^{\infty} A_{l+n-m,n} B_{l+n,m-n} \\ &= \sum_{n'=-\infty}^{\infty} A_{l+n',n'+m} B_{l+m+n',-n'}, \end{aligned} \quad (16)$$

where the last equality is completed with $n' = n - m$. We now complete an index transformation, such that $A_{i,j} \rightarrow \mathcal{A}_{r,s}$, where $r = (i - j)/2$ and $s = (i + j)/2$:

$$\mathcal{C}_{r,s} = \sum_{n'=-\infty}^{\infty} \mathcal{A}_{r,n'+s} \mathcal{B}_{n'+s,s} = \sum_{n=-\infty}^{\infty} \mathcal{A}_{r,n} \mathcal{B}_{n,s}, \quad (17)$$

where the last equality has a shift in the infinite summation. With the assumption of periodicity, the above convolution has been brought to the form of a matrix equation. These matrices (the Floquet matrices), with indices running from negative infinity to infinity, take the following form in terms of the original Fourier components:

$$\mathcal{A} = \begin{pmatrix} \dots & \dots & \dots & \dots & \dots \\ \dots & A(\omega - \Omega, 0) & A(\omega - \frac{\Omega}{2}, 1) & A(\omega, 2) & \dots \\ \dots & A(\omega - \frac{\Omega}{2}, -1) & A(\omega, 0) & A(\omega + \frac{\Omega}{2}, 1) & \dots \\ \dots & A(\omega, -2) & A_{i,j}(\omega + \frac{\Omega}{2}, -1) & A(\omega + \Omega, 0) & \dots \\ \dots & \dots & \dots & \dots & \dots \end{pmatrix}. \quad (18)$$

In the context of the problem, the elements of the Floquet matrices are the Fourier coefficients of the Green's function or the lead self-energies in Keldysh-Schwinger space, themselves matrices of $2n$ dimensions. Via a unitary transformation, the elements within the Floquet matrices can be rearranged. As a consequence, they can be brought to look like the matrices one would expect in the static case, but with the innermost elements being infinite matrices populated by Fourier coefficients, as opposed to a scalar within the static case.

Generally, to solve for the inverses of the Floquet matrices, one must truncate the matrices at a large enough

dimension to have a negligible effect on the calculations. Removing all time dependence, the matrices reduce to scalars, agreeing with the static case results.

We also have to consider the following limiting cases of Eq. (13):

$$C(t, t') = A(t)B(t, t'), \quad (19)$$

which follows from $A(t, t') \rightarrow A(t)\delta(t - t')$. Therefore, given the application of Eq. (12), the above has the same form as in Eq. (17), with the Floquet matrix of \mathcal{A} populated with the Fourier coefficient of $A(t)$.

Solving the Kadanoff-Baym equations by invoking a

Floquet approach restricts the method to considering time-averaged statistics: the points of measurement are moved to the infinities to ensure the periodicity of the system (i.e., $t_0 \rightarrow -\infty$ and $t_c \rightarrow \infty$). Following the above considerations, the Kadanoff-Baym equation can be transformed into a matrix equation:

$$\left[\begin{pmatrix} \omega \mathbf{I} & 0 \\ 0 & \omega \mathbf{I} \end{pmatrix} + \begin{pmatrix} \Omega \mathbf{D} & 0 \\ 0 & \Omega \mathbf{D} \end{pmatrix} - \begin{pmatrix} \mathbf{H} & 0 \\ 0 & \mathbf{H} \end{pmatrix} - \begin{pmatrix} \Sigma^{\mathbf{T}} & \Sigma^{\mathbf{<}} \\ -\Sigma^{\mathbf{>}} & -\Sigma^{\tilde{\mathbf{T}}} \end{pmatrix} \right] \check{\mathcal{G}} = \begin{pmatrix} \mathbf{I} & 0 \\ 0 & \mathbf{I} \end{pmatrix}, \quad (20)$$

where $(\mathbf{D})_{a,b} = a\delta_{a,b}$, $(\mathbf{H})_{a,b} = \mathbf{h}(b-a)$, and the elements of the self-energy are given as

$$(\Sigma)_{a,b} = \Sigma(\omega + (a+b)\Omega/2, b-a), \quad (21)$$

for a given projection. See the Appendix for calculations of the self-energies.

One can recast Eq. (7) in terms of Floquet matrices, giving us

$$\begin{aligned} C_n &= \lim_{t_c, t_0 \rightarrow \pm\infty} \left(\frac{(-i)^n \frac{\partial^n}{\partial \lambda^n} \ln[\chi(\lambda_L, t_c, t_0)]}{t_c - t_0} \right) \\ &= (-i)^{n-1} \frac{\partial^{n-1}}{\partial \lambda^{n-1}} \int_{-\infty}^{\infty} \frac{d\omega}{2\pi} \text{Tr}[X(\omega, 0)], \end{aligned} \quad (22)$$

where $n \geq 1$ and $X(\omega, 0)$ is the zeroth Fourier component, calculated from the Floquet matrix equation

$$\mathbf{X} = \Sigma_{<}^L \mathcal{G}_{>} - \mathcal{G}_{<} \Sigma_{>}^L. \quad (23)$$

This result corresponds to calculating the time-averaged cumulants of the current, with $C_1 = I$ and $C_2 = S_{LL}(\omega = 0)$ ^{68,80}.

III. APPLICATION

A. Resonant level

We begin by considering a central region consisting of a single resonant level. The central region and leads are both taken to have sinusoidal driving. The central region Hamiltonian is

$$H_C(t) = [\epsilon_0 + \Delta_0 \cos(\Omega t)] d^\dagger d, \quad (24)$$

and the leads' energy levels are

$$\epsilon_{k\alpha}(t) = \epsilon_{k\alpha} + \Delta_\alpha \cos(\Omega t). \quad (25)$$

For the details of the derivations for the time-dependent lead self-energies, see the Appendix.

Considering the current, one can turn off the counting field and rearrange Eq. (22) to find

$$\begin{aligned} I &= \sum_{k=-\infty}^{\infty} \int_{-\infty}^{\infty} \frac{d\omega}{2\pi} T(\omega - k\Omega) \\ &\times \left(f_L(\omega) J_k^2 \left(\frac{\Delta_0 - \Delta_L}{\Omega} \right) - f_R(\omega) J_k^2 \left(\frac{\Delta_0 - \Delta_R}{\Omega} \right) \right) \end{aligned} \quad (26)$$

where

$$T(\omega) = \frac{\Gamma_L \Gamma_R}{(\omega - \epsilon_0)^2 + \frac{\Gamma^2}{4}}, \quad (27)$$

in agreement with the literature^{30,75}. We see the established phenomena of photon-assisted transport, where the sinusoidal driving of regions results in an effective splitting of the transmission between pictures which can be interpreted as the absorption or emission of photons of $\hbar\Omega$ ¹.

The results of these calculations are given in Figs. 1 and 2. Within all the calculations completed, the matrices were truncated to consider 41 of the Fourier coefficients of each object (i.e., from $n = -20$ to $n = 20$). We see that the higher cumulants also display characteristics surrounding the positions of the photopeaks. With the photopeaks entering into the voltage window, the cumulants C_2 and C_3 decrease in magnitude, suggesting that the moving of the photopeaks into resonance decreases the variability within the average current. Indeed, as the photopeaks move into the resonance, the ratio C_2/C_1 , an appropriate indicator for the clarity of the current, decreases. This is expected, with increasing voltage, moving the effects of the driving further away, as the level moves further into resonance.

For C_3 , as the photopeak approaches the voltage window, we see an increase, followed by a decrease, when the photopeak has entered into the voltage window. The above suggests that, around voltages where photopeaks are entering resonance, the current suffers an increased skewness in its distribution. This can be seen with the ratio of C_3/C_1 , which is larger than in the static case (see Fig. 2), within the region before the first photopeak enters resonance.

B. Quantum interference

Within the central junction, effects due to interference between many levels can give rise to interesting and complicated phenomena⁸¹. In particular, many-level systems, often containing Aharonov-Bohm interference effects, have been studied with time-dependent drivings^{29,32,56,75,82-92}. Here, we investigate a simple manifestation of Fano interference due to a secondary offset level coupled to our primary site but uncoupled from the electrodes. The introduction of this secondary

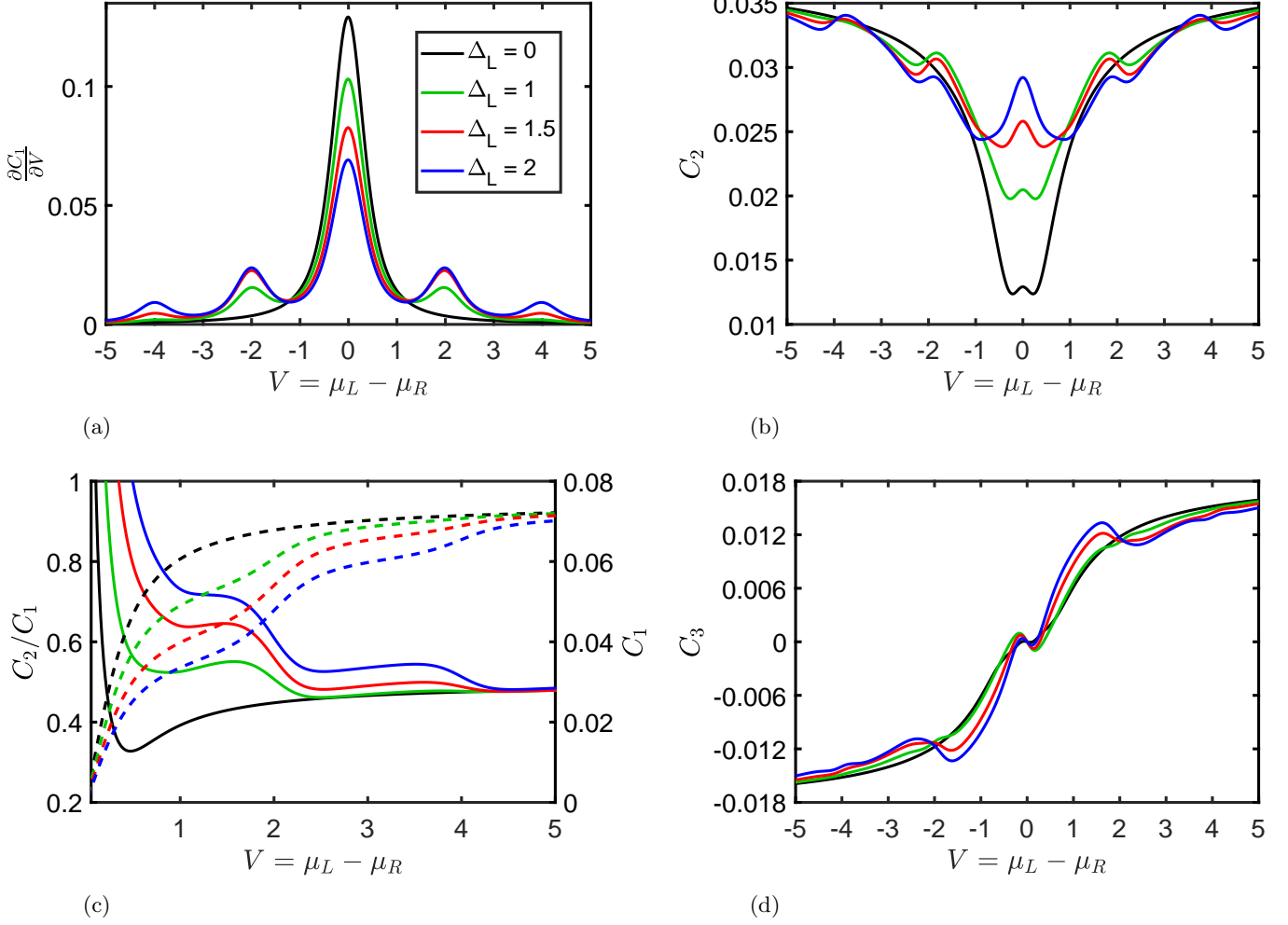


FIG. 1: Cumulants of the current plotted against increasing voltage ($\mu_L = -\mu_R$) for a single level. The left lead's driving is increased, revealing the effects of the photopeaks. Dashed lines shows C_1 , and solid lines show C_2/C_1 in (c). The parameters are $\Gamma_L = \Gamma_R = 0.15$, $\varepsilon_1 = 0$, $T = 0.05$, $\Omega = 1$, $\Delta_0 = 0$, and $\Delta_R = 0$.

site results in interference between the two paths through the system. The Hamiltonian for the central region is

$$H_C = \varepsilon_1 d_1^\dagger d_1 + \varepsilon_0 d_0^\dagger d_0 + t(d_1^\dagger d_0 + d_0^\dagger d_1), \quad (28)$$

and the central region is connected to the leads through level ε_0

$$H_{CL} + H_{CR} = \sum_{i,k,\alpha=L,R} (t_{k\alpha} c_{k\alpha}^\dagger d_0 + \text{H.c.}). \quad (29)$$

The leads are sinusoidally driven as in the resonant level case considered before Eq. (25), and the central region Hamiltonian remains static all the time.

Calculations for the current concur with theory [Eq. (26)], with the transmission undergoing well-known changes due to the introduction of the second level⁸¹:

$$T(\omega) = \frac{\Gamma_L \Gamma_R}{[\omega - \varepsilon_0 - t^2/(\omega - \varepsilon_1)]^2 + \frac{\Gamma^2}{4}}. \quad (30)$$

The results of the calculations are given in Fig. 3. With the introduction of the secondary level, the photon-assisted sidebands in the current acquire pronounced asymmetrical interference patterns from the Fano resonance [see Fig. 3a], with the asymmetry being governed by the difference between the energies of the levels. Moreover, the asymmetric feature manifests in the central peak differently from within the photopeaks, with a change in the difference in the levels' energies pushing the feature in the opposite direction for the photopeaks compared to the central peak.

To understand the effects of the secondary level, one can diagonalize the central region Hamiltonian, allowing for the investigation of the current in terms of the bonding (-) and antibonding (+) molecular orbitals⁹³, which gives the energies

$$\varepsilon_{\pm} = \frac{1}{2} \left(\varepsilon_0 + \varepsilon_1 \pm \sqrt{(\varepsilon_0 - \varepsilon_1)^2 + 4t^2} \right) \quad (31)$$

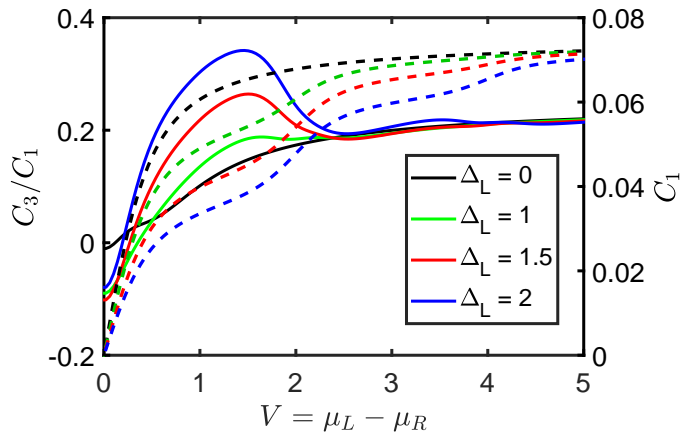


FIG. 2: The ratio of cumulants, C_3/C_1 plotted against increasing voltage ($\mu_L = -\mu_R$) for a single level.

Dashed lines shows C_1 , and solid lines show C_3/C_1 . The left lead's driving is increased, revealing the effects of the photopeaks. The parameters are those of Fig. 1.

and a modified linewidth function:

$$\tilde{\Gamma}_{i,j}^\alpha = \Gamma^\alpha \begin{pmatrix} \cos^2(\beta) & \cos(\beta)\sin(\beta) \\ \cos(\beta)\sin(\beta) & \sin^2(\beta) \end{pmatrix}, \quad (32)$$

where

$$\beta = \frac{1}{2} \tan^{-1} \left(\frac{2t}{\epsilon_0 - \epsilon_1} \right). \quad (33)$$

The diagonalization of the central region allows us to identify the roles that the bonding and antibonding molecular levels play in the cumulants. Furthermore, the effects due to the interaction between these levels is relegated to the off-diagonal terms of the linewidth function [Eq. (32)], with their removal corresponding to a system without interaction between the bonding and antibonding levels.

The effects of the separation into the bonding and antibonding levels can be seen within Fig. 4. Here, the contributions by both levels are plotted for the case where the off-diagonals within the modified linewidth function [i.e. Eq. (32)] are disregarded. We see that the contributions from the diagonalized levels approximately explain the positions of the peaks within the differential conductance, with the off diagonal terms of the modified linewidth varying the final positions slightly. This analysis also helps to explain the features of the higher cumulants in terms of the bonding and antibonding molecular levels.

The effects of the asymmetrical feature due to the Fano resonance can be seen to effect the higher cumulants [see Fig. 3b and 3d]. While this complicates the features of the cumulants, it was found to not alter the junction's dynamics significantly. This is evident in $F_2 = C_2/C_1$ [see Fig. 3c], which suggests no significant changes in the efficiency of the device, with the introduction of a second

level resulting in a splitting of the plateauing effect, seen in Fig. 1c, due to the shared influence of the bonding and antibonding levels.

IV. DISCUSSION AND CONCLUSION

The method investigated allows for the calculation of the time-averaged cumulants of the current for periodically driven molecular junctions. Expressing the Green's functions in terms of a Fourier series allows for the equation of motion to be cast as a matrix equation of infinite dimensions, which, following truncation, can be easily solved. The method was applied to investigate the time-averaged current cumulants for both a single-level system and a T-shaped double-level system. In investigating the higher cumulants the derivatives of the counting field were evaluated with the finite central difference method.

The method is applicable to many levels, and the wide-band approximation is not essential. Furthermore, its application to systems considering extra correlations is conceivable.

It should be noted that the above method calculates the time averages of the cumulants of the current. These calculations should not be confused with the statistics one could calculate when considering the distribution of instantaneous values (for current, noise, etc.) that could be calculated within a period of the driving. While the latter would be more appropriate if one were interested in the instantaneous measurements, the former is more appropriate for devices which would cumulate large transmitted charges before measurement.

Within the investigation, it was found that the time-dependent driving of the leads not only induces photopeaks within the current but also generates features within the higher cumulants. The positioning of photopeaks relative to the voltage window was found to have a significant effect on the higher cumulants. Photopeaks that sit just outside resonance have the effect of increasing both the second and third cumulants, while photopeaks that sit just within resonance see a relative decrease in both cumulants. Furthermore, it was found that the time-dependent driving broadened and skewed the current distribution. This was observable within C_2/C_1 and C_3/C_1 [see Figs. 1c and 2 respectively].

Even within the reduced picture of considering time averages, it is evident that the effects of time-dependent driving go beyond the current. This suggests that further investigations into the cumulants of important observables will be essential for understanding time-dependent driven systems.

On top of this, methods that can be extended to consider extra correlations (i.e., electron-phonon and electron-electron interactions) will allow for a fuller understanding of time-dependent driven molecular junctions as they are truly realized, which will hopefully lead to further interesting results.

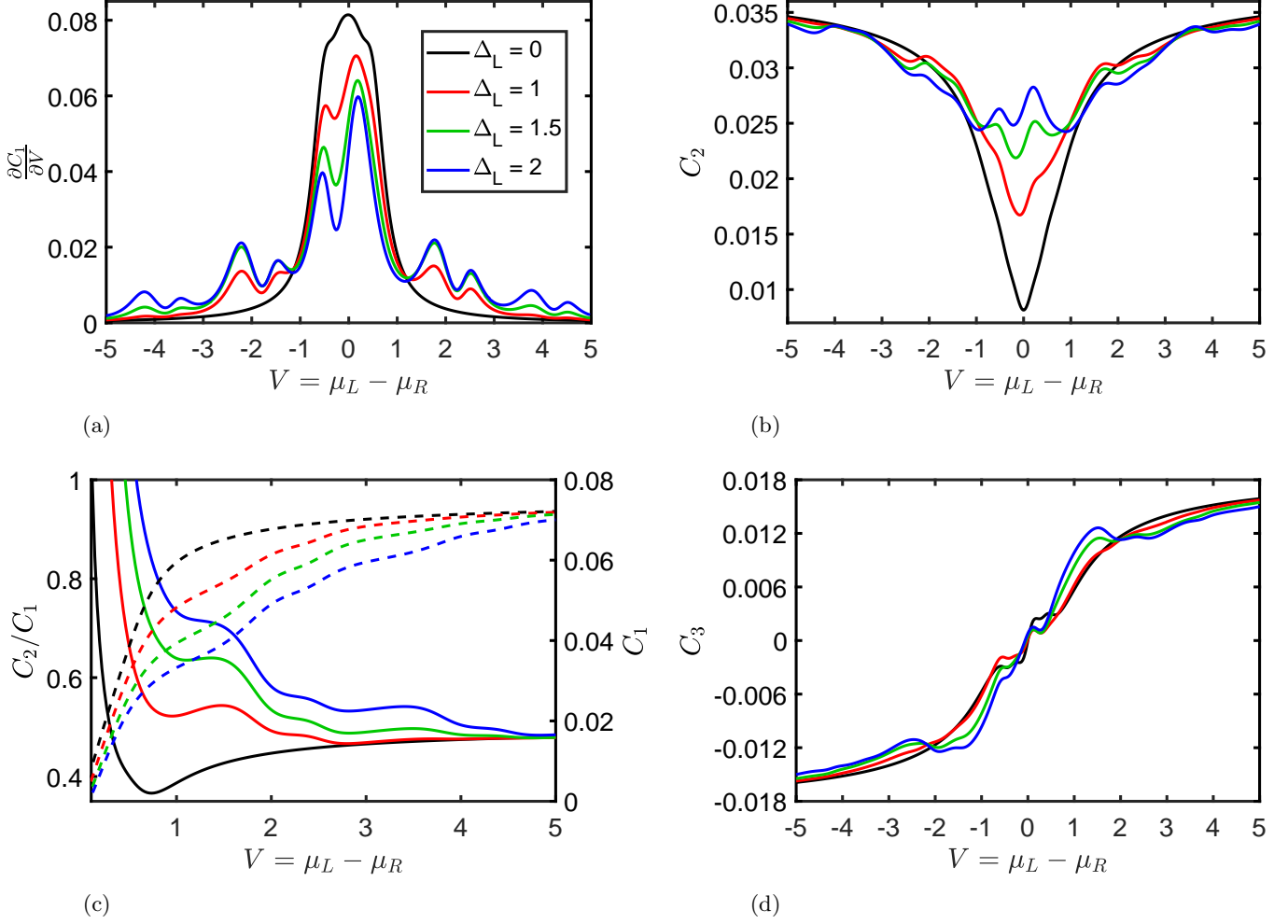


FIG. 3: Cumulants of the current plotted against increasing voltage ($\mu_L = -\mu_R$). The leads are connected to the first level, which is further connected to the isolated second level. Dashed lines shows C_1 , and solid lines show C_2/C_1 in (c). Here, the left lead's driving is increased to reveal the effects of the Fano interference on the photopeaks and higher cumulants. The parameters are $\Gamma_L = \Gamma_R = 0.15$, $\varepsilon_0 = 0$, $\varepsilon_1 = 0.15$, $t = 0.15$, $T = 0.05$, $\Omega = 1$, and $\Delta_R = 0$.

Appendix A: Lead self-energies with the AC driving

The lead self-energies are given as

$$\Sigma_{\alpha,ij}^{<,>,T,\tilde{T}}(t,t') = \sum_{k,k'} t_{k\alpha,i}^* g_{k\alpha,k'\alpha}^{<,>,T,\tilde{T}}(t,t') t_{k'\alpha,j}(t'), \quad (\text{A1})$$

where

$$g_{k\alpha,k'\alpha}^{<}(t,t') = i f_{k\alpha} e^{-i \int_{t'}^t dt_1 \varepsilon_{k\alpha}(t_1)} \delta_{k,k'}, \quad (\text{A2})$$

$$g_{k\alpha,k'\alpha}^{>}(t,t') = -i(1 - f_{k\alpha}) e^{-i \int_{t'}^t dt_1 \varepsilon_{k\alpha}(t_1)} \delta_{k,k'}, \quad (\text{A3})$$

$$g_{k,k'}^T(t,t') = g_{k\alpha,k'\alpha}^{>}(t,t') \Theta(t-t') + g_{k\alpha,k'\alpha}^{<}(t,t') \Theta(t'-t), \quad (\text{A4})$$

$$g_{k,k'}^{\tilde{T}}(t,t') = g_{k\alpha,k'\alpha}^{<}(t,t') \Theta(t-t') + g_{k\alpha,k'\alpha}^{>}(t,t') \Theta(t'-t). \quad (\text{A5})$$

The Fermi-Dirac occupation is given by the standard definition:

$$f_{k\alpha} = \frac{1}{1 + e^{(\varepsilon_{k\alpha} - \mu_\alpha)/T_\alpha}}. \quad (\text{A6})$$

Within the investigation, we assume sinusoidal driving within the leads,

$$\varepsilon_{k\alpha}(t) = \varepsilon_{k\alpha} + \Delta_\alpha \cos(\Omega_\alpha t), \quad (\text{A7})$$

and that the couplings to the leads are constant. We can collect the terms together, making use of the definition for the self energy in the static case (denoted with

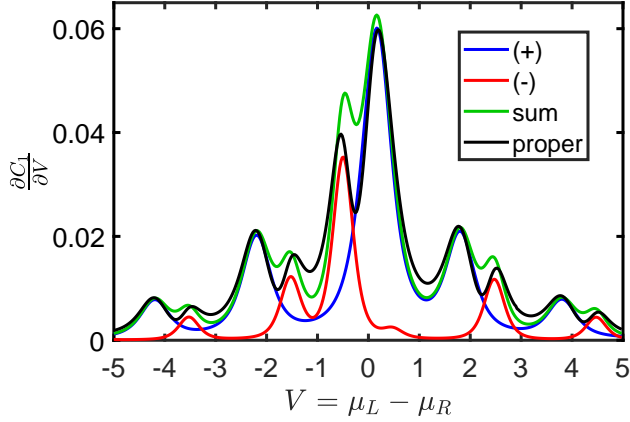


FIG. 4: The differential conductance plotted against increasing voltage ($\mu_L = -\mu_R$). The leads are connected to the first level, which is further connected to the isolated second level. Here, the bonding and antibonding levels are plotted, disregarding the off-diagonal terms within the diagonalized linewidth function [Eq. 32], along with their sum and the full result, which does include the off-diagonal terms. The parameters are $\Gamma_L = \Gamma_R = 0.15$, $\varepsilon_0 = 0$, $\varepsilon_1 = 0.15$, $t = 0.15$, $T = 0.05$, $\Omega = 1$, and $\Delta_R = 0$.

an apostrophe):

$$\begin{aligned} \Sigma_{\alpha,ij}(t,t') &= \Sigma'_{\alpha,ij}(t-t')e^{-i\int_{t'}^t dt_1 \Delta_\alpha \cos(\Omega_\alpha t_1)} \\ &= e^{-i\frac{\Delta_\alpha}{\Omega_\alpha} \sin(\Omega_\alpha t)} \Sigma'_{\alpha,ij}(t-t') e^{i\frac{\Delta_\alpha}{\Omega_\alpha} \sin(\Omega_\alpha t')}. \end{aligned} \quad (\text{A8})$$

We see that the above follows a pattern similar to Eq. (13) and, following a similar analysis, can be expressed as the matrix multiplication of three Floquet matrices:

$$\Sigma_{\alpha,ij} = \mathcal{S} \Sigma'_{\alpha,ij} \mathcal{S}^\dagger. \quad (\text{A9})$$

Here, \mathcal{S} is found with the use of the Jacobi-Anger expansion:

$$e^{iz \sin(\theta)} = \sum_{n=-\infty}^{n=\infty} J_n(z) e^{in\theta}, \quad (\text{A10})$$

such that $\mathcal{S}_{s,r} = J_{s-r}(\Delta_\alpha/\Omega_\alpha)$. Here, $J_n(x)$ are Bessel functions of the first kind.

-
- ¹ G. Platero and R. Aguado, *Physics Reports* **395**, 1 (2004).
- ² C. Meyer, J. M. Elzerman, and L. P. Kouwenhoven, *Nano Letters* **7**, 295 (2007).
- ³ M. Chauvin, P. vom Stein, H. Pothier, P. Joyez, M. E. Huber, D. Esteve, and C. Urbina, *Phys. Rev. Lett.* **97**, 067006 (2006).
- ⁴ H. K. Yadalam and U. Harbola, *Phys. Rev. B* **93**, 035312 (2016).
- ⁵ A. Croy and U. Saalman, *Phys. Rev. B* **93**, 165428 (2016).
- ⁶ P. Haughian, H. H. Yap, J. Gong, and T. L. Schmidt, *Phys. Rev. B* **96**, 195432 (2017).
- ⁷ Y. Selzer and U. Peskin, *The Journal of Physical Chemistry C* **117**, 22369 (2013).
- ⁸ M. A. Ochoa, Y. Selzer, U. Peskin, and M. Galperin, *The Journal of Physical Chemistry Letters* **6**, 470 (2015).
- ⁹ X. W. Tu, J. H. Lee, and W. Ho, *J. Chem. Phys.* **124**, 021105 (2006).
- ¹⁰ J. Trasobares, D. Vuillaume, D. Théron, and N. Clément, *Nature Communications* **7**, 12850 (2016).
- ¹¹ P. K. Tien and J. P. Gordon, *Phys. Rev.* **129**, 647 (1963).
- ¹² A. H. Dayem and R. J. Martin, *Phys. Rev. Lett.* **8**, 246 (1962).
- ¹³ M. H. Pedersen and M. Büttiker, *Phys. Rev. B* **58**, 12993 (1998).
- ¹⁴ M. Grifoni and P. Hänggi, *Physics Reports* **304**, 229 (1998).
- ¹⁵ S. Camalet, J. Lehmann, S. Kohler, and P. Hänggi, *Phys. Rev. Lett.* **90**, 210602 (2003).
- ¹⁶ S. Kohler, J. Lehmann, and P. Hänggi, *Physics Reports* **406**, 379 (2005).
- ¹⁷ B. Trauzettel, Y. M. Blanter, and A. F. Morpurgo, *Phys. Rev. B* **75**, 035305 (2007).
- ¹⁸ M. Moskalets and M. Büttiker, *Phys. Rev. B* **66**, 205320 (2002).
- ¹⁹ M. Moskalets and M. Büttiker, *Phys. Rev. B* **69**, 205316 (2004).
- ²⁰ M. V. Moskalets, *Scattering Matrix Approach to Non-stationary Quantum Transport* (World Scientific, 2012).
- ²¹ M. F. Ludovico, J. S. Lim, M. Moskalets, L. Arrachea, and D. Sánchez, *Phys. Rev. B* **89**, 161306 (2014).
- ²² A. Purkayastha and Y. Dubi, *Phys. Rev. B* **96**, 085425 (2017).
- ²³ U. Peskin, *Fortschritte der Physik* **65**, 1600048 (2017).
- ²⁴ L. Arrachea, *Phys. Rev. B* **72**, 125349 (2005).
- ²⁵ L. Arrachea and M. Moskalets, *Phys. Rev. B* **74**, 245322 (2006).
- ²⁶ S.-H. Ke, R. Liu, W. Yang, and H. U. Baranger, *J. Chem. Phys.* **132**, 234105 (2010).
- ²⁷ R. Tuovinen, E. Peretto, G. Stefanucci, and R. van Leeuwen, *Phys. Rev. B* **89**, 085131 (2014).
- ²⁸ B. Wang, J. Wang, and H. Guo, *Phys. Rev. Lett.* **82**, 398 (1999).
- ²⁹ Q.-f. Sun, J. Wang, and T.-h. Lin, *Phys. Rev. B* **58**, 13007 (1998).
- ³⁰ A.-P. Jauho, N. S. Wingreen, and Y. Meir, *Phys. Rev. B* **50**, 5528 (1994).
- ³¹ S. Datta and M. P. Anantram, *Phys. Rev. B* **45**, 13761 (1992).
- ³² C. A. Stafford and N. S. Wingreen, *Phys. Rev. Lett.* **76**, 1916 (1996).
- ³³ T. Brandes, *Phys. Rev. B* **56**, 1213 (1997).
- ³⁴ G. Stefanucci and C.-O. Almbladh, *Phys. Rev. B* **69**, 195318 (2004).
- ³⁵ H. M. Pastawski, *Phys. Rev. B* **46**, 4053 (1992).
- ³⁶ L. Y. Chen and C. S. Ting, *Phys. Rev. B* **43**, 2097 (1991).
- ³⁷ J. Maciejko, J. Wang, and H. Guo, *Phys. Rev. B* **74**, 085324 (2006).
- ³⁸ Y. Zhu, J. Maciejko, T. Ji, H. Guo, and J. Wang, *Phys. Rev. B* **71**, 075317 (2005).
- ³⁹ M. Ridley, A. MacKinnon, and L. Kantorovich, *Phys. Rev. B* **91**, 125433 (2015).
- ⁴⁰ M. Ridley, A. MacKinnon, and L. Kantorovich, *Phys. Rev. B* **95**, 165440 (2017).
- ⁴¹ M. Vanević, Y. V. Nazarov, and W. Belzig, *Phys. Rev. Lett.* **99**, 076601 (2007).
- ⁴² M. F. Ludovico, F. Battista, F. von Oppen, and L. Arrachea, *Phys. Rev. B* **93**, 075136 (2016).
- ⁴³ D. Kienle, M. Vaidyanathan, and F. Léonard, *Phys. Rev. B* **81**, 115455 (2010).
- ⁴⁴ Q.-f. Sun and T.-h. Lin, *Phys. Rev. B* **56**, 3591 (1997).
- ⁴⁵ T. D. Honeychurch and D. S. Kosov, *Phys. Rev. B* **100**, 245423 (2019).
- ⁴⁶ T. Kwapiński, R. Taranko, and E. Taranko, *Phys. Rev. B* **66**, 035315 (2002).
- ⁴⁷ R. Taranko, T. Kwapiński, and E. Taranko, *Phys. Rev. B* **69**, 165306 (2004).
- ⁴⁸ T. Kwapiński, R. Taranko, and E. Taranko, *Phys. Rev. B* **72**, 125312 (2005).
- ⁴⁹ J. P. Pekola, O.-P. Saira, V. F. Maisi, A. Kemppinen, M. Möttönen, Y. A. Pashkin, and D. V. Averin, *Rev. Mod. Phys.* **85**, 1421 (2013).
- ⁵⁰ T. J. Suzuki and T. Kato, *Phys. Rev. B* **91**, 165302 (2015).
- ⁵¹ Z. Feng, J. Maciejko, J. Wang, and H. Guo, *Phys. Rev. B* **77**, 075302 (2008).
- ⁵² Z. Ma, Y. Zhu, X.-Q. Li, T.-h. Lin, and Z.-B. Su, *Phys. Rev. B* **69**, 045302 (2004).
- ⁵³ Q. Chen and H. K. Zhao, *European Physical Journal B* **64**, 237 (2008).
- ⁵⁴ Q.-f. Sun, J. Wang, and T.-h. Lin, *Phys. Rev. B* **61**, 13032 (2000).
- ⁵⁵ H.-K. Zhao and J. Wang, *The European Physical Journal B* **59**, 329 (2007).
- ⁵⁶ H.-K. Zhao and L.-L. Zhao, *The European Physical Journal B* **79**, 485 (2011).
- ⁵⁷ B. H. Wu and J. C. Cao, *Phys. Rev. B* **81**, 085327 (2010).
- ⁵⁸ B. H. Wu and C. Timm, *Phys. Rev. B* **81**, 075309 (2010).
- ⁵⁹ L. Levitov and G. Lesovik, *JETP Lett.* **58**, 230 (1993).
- ⁶⁰ L. S. Levitov, H. Lee, and G. B. Lesovik, *Journal of Mathematical Physics* **37**, 4845 (1996).
- ⁶¹ M. Esposito, U. Harbola, and S. Mukamel, *Rev. Mod. Phys.* **81**, 1665 (2009).
- ⁶² Y. V. Nazarov and Y. M. Blanter, *Quantum Transport: Introduction to Nanoscience* (Cambridge University Press, 2009).
- ⁶³ D. A. Ivanov, H. W. Lee, and L. S. Levitov, *Phys. Rev. B* **56**, 6839 (1997).
- ⁶⁴ J. Zhang, Y. Sherkunov, N. d'Ambrumenil, and B. Muzykantskii, *Phys. Rev. B* **80**, 245308 (2009).
- ⁶⁵ D. A. Ivanov and A. G. Abanov, *EPL (Europhysics Letters)* **92**, 37008 (2010).
- ⁶⁶ M. Benito, M. Niklas, and S. Kohler, *Phys. Rev. B* **94**, 195433 (2016).

- ⁶⁷ Y. . Zheng and F. L. H. Brown, *The Journal of Chemical Physics* **139**, 164120 (2013).
- ⁶⁸ J. Fransson and M. Galperin, *Phys. Rev. B* **81**, 075311 (2010).
- ⁶⁹ T.-H. Park and M. Galperin, *Phys. Rev. B* **84**, 205450 (2011).
- ⁷⁰ A. Ueda, Y. Utsumi, Y. Tokura, O. Entin-Wohlman, and A. Aharony, *J. Chem. Phys.* **146**, 092313 (2017).
- ⁷¹ R. Avriller and A. Levy Yeyati, *Phys. Rev. B* **80**, 041309 (2009).
- ⁷² T. L. Schmidt and A. Komnik, *Phys. Rev. B* **80**, 041307 (2009).
- ⁷³ A. O. Gogolin and A. Komnik, *Phys. Rev. B* **73**, 195301 (2006).
- ⁷⁴ M. Ridley, V. N. Singh, E. Gull, and G. Cohen, *Phys. Rev. B* **97**, 115109 (2018).
- ⁷⁵ G.-M. Tang and J. Wang, *Phys. Rev. B* **90**, 195422 (2014).
- ⁷⁶ Z. Yu, G.-M. Tang, and J. Wang, *Phys. Rev. B* **93**, 195419 (2016).
- ⁷⁷ G. Cabra, I. Franco, and M. Galperin, *The Journal of Chemical Physics* **152**, 094101 (2020).
- ⁷⁸ N. Tsuji, T. Oka, and H. Aoki, *Phys. Rev. B* **78**, 235124 (2008).
- ⁷⁹ J. Rammer, *Quantum Field Theory of Non-equilibrium States* (Cambridge University Press, 2007).
- ⁸⁰ D. Kambly and C. Flindt, *Journal of Computational Electronics* **12**, 331 (2013).
- ⁸¹ J. C. Cuevas and E. Scheer, *Molecular Electronics: An Introduction to Theory and Experiment*, EBSCO ebook academic collection (World Scientific Publishing Company Pte Limited, 2010).
- ⁸² T. Fujisawa and S. Tarucha, *Japanese Journal of Applied Physics* **36**, 4000 (1997).
- ⁸³ B. H. Wu and J. C. Cao, *Phys. Rev. B* **73**, 205318 (2006).
- ⁸⁴ J. Bai, L. Li, Z. He, S. Ye, S. Zhao, S. Dang, and W. Sun, *Chinese Physics B* **26**, 117302 (2017).
- ⁸⁵ Z. He, J. Bai, L. Li, Q. Zhi, and W. Sun, *Moscow University Physics Bulletin* **73**, 486 (2018).
- ⁸⁶ T. H. Oosterkamp, T. Fujisawa, W. G. van der Wiel, K. Ishibashi, R. V. Hijman, S. Tarucha, and L. P. Kouwenhoven, *Nature* **395**, 873 (1998).
- ⁸⁷ H. Pan, S.-Q. Duan, W.-D. Chu, and W. Zhang, *Physics Letters A* **372**, 3292 (2008).
- ⁸⁸ R. Shang, H.-O. Li, G. Cao, M. Xiao, T. Tu, H. Jiang, G.-C. Guo, and G.-P. Guo, *Applied Physics Letters* **103**, 162109 (2013).
- ⁸⁹ B.-C. Wang, G. Cao, B.-B. Chen, G.-D. Yu, H.-O. Li, M. Xiao, and G.-P. Guo, *Journal of Applied Physics* **120**, 064302 (2016).
- ⁹⁰ Z. Zhao, Y. Min, and Y. Huang, *Physica E: Low-dimensional Systems and Nanostructures* **114**, 113589 (2019).
- ⁹¹ X. Zhao, R.-Y. Yuan, A.-C. Ji, H. Yan, and Y. Guo, *Journal of Applied Physics* **116**, 103517 (2014).
- ⁹² X. Zhao, R. Yuan, H. Yan, and Y. Guo, *Physica B: Condensed Matter* **443**, 84 (2014).
- ⁹³ H. Lu, R. Lü, and B.-f. Zhu, *Phys. Rev. B* **71**, 235320 (2005).